AN (ITO OR AZO)/ZnO/Cu($In_{1-x}Ga_x$)Se_2 SUPERSTRATE THIN FILM SOLAR CELL STRUCTURE PREPARED BY SPRAY PYROLYSIS

B. J. Babu, S. Velumani and R. Asomoza
Department of Electrical Engineering-SEES, CINVESTAV-IPN, Zacatenco, Mexico D.F., C.P. 07360, Mexico

ABSTRACT

Feasibility of preparing a thin film (ITO or AZO)/ZnO/Cu($In_{1-x}Ga_x$)Se_2 (CIGS) heterojunction solar cell using low cost non-vacuum technique is demonstrated. Low resistive (10^{-4} Ohm-cm) Indium tin oxide (ITO) (>80%T) and ZnO:Al (AZO) (10^{-3} Ohm-cm) (>75%T) films of ~700 nm thickness were deposited on to glass substrates using Ultrasonic Spray Pyrolysis (USP) at 420°C and 475°C respectively. Over this a 300 nm i-ZnO buffer layer was deposited at 400°C by USP. XRD and optical data results indicates that ITO and AZO, i-ZnO crystallites exhibits cubic and hexagonal wurtizite structures with direct band gap of 3.75 and 3.32, 3.31 eV respectively. FE-SEM analysis showed pyramidal and columnar structure for ITO and AZO, i-ZnO. Composition obtained from EDAX showed the amount of tin and aluminum doped into the ITO and AZO films. Little or no interdiffusion was found at the ITO/ZnO interface, allowing the use of high temperatures for deposition. Preliminary depositions of Cu($In_{1-x}Ga_x$)Se_2 (x=1 to 0) layer over glass showed polycrystalline chalcopyrite in nature with preferred (112) orientation. Raman studies showed a peak corresponding to A1 mode CIGS phase at ~170 cm^{-1}. A 700 nm graded CIGS layer showed high optical absorption coefficient value of 10^6 cm^{-1} with a band gap of 1.25 eV. Graded CIGS layer was deposited over ITO/ZnO and AZO/ZnO layers at a substrate temperature of 350^0C after an appropriate surface treatment. XRD/FESEM analyses revealed the crystallinity and graded distribution of gallium and indium.

INTRODUCTION

Thin film solar cells based on the chalcopyrite material Cu(In, Ga)Se_2 (CIGS) have received considerable attention due to their high absorption coefficient (>10^5 cm^{-1}) and the potential for low cost manufacturing, recently CIGS thin film solar cells approached efficiencies of 20.3% [1] for substrate configuration of glass/Mo/CIGS/CdS/AZO. An alternate design is the superstrate configuration, where the deposition sequence is reversed; thus, the absorber is grown on glass coated with the transparent front contact and finished by an evaporated metal back contact. Solar cells in this configuration offer the advantage of easy and reliable encapsulation; furthermore, they are important for the development of advanced tandem solar cells [2]. Several papers to date have reported on the fabrication of CIGS [3, 4] and CIS [5] thin film solar cells using this device structure. An efficiency of 12.8% has been reported for superstrate solar cells prepared with co-evaporated Na_2S as a source of Na doping in CIGS [3]. Low efficiencies of superstrate CIGS cells are attributed to undesired inter-diffusion at the CdS/CIGS interface during higher temperature deposition of CIGS. Nakada et al. [2] replaced the CdS buffer layer with a ZnO film, which significantly reduced the interface diffusion. Among thin film techniques, spray pyrolysis has many advantages over other non-vacuum techniques such as large area deposition, low cost, material efficient process. In_2O_3:Sn and ZnO:Al has been widely used as a window material but there seems to be some doubt about the stoichiometric stability of In_2O_3:Sn material for long-term operation because of its porosity. In contrast, ZnO is an n-type material with a highly stable band gap (3.3 eV) and it can be prepared by a simple technique such as spray pyrolysis [5, 6]. Very few authors reported formation of CIS layer over ZnO [5] and deposition of CIGS over glass using spray pyrolysis [7-10]. In the present work we demonstrated deposition and characterization of ITO/ZnO, AZO/ZnO junctions by USP, Cu($In_{1-x}Ga_x$)Se_2 layers by pneumatic spray system and their heterojunction solar cell prepared entirely by spray pyrolysis. Also for first time we report deposition of graded CIGS layer by chemical spray pyrolysis.

EXPERIMENTAL PROCEDURE

Superstrate-type CIGS solar cell with glass/(ITO or ZnO:Al)/ZnO/CIGS structure (see Fig. 1) is prepared by spray pyrolysis. Approximately 700 nm thick Indium-Tin-Oxide (ITO) and Al-doped ZnO (AZO) thin films were deposited on to glass substrates using USP at 420°C and 475°C respectively. After this a 300 nm i-ZnO buffer layers was deposited on to it at a substrate temperature of 400°C by USP from zinc acetate precursor. Resistivity, mobility, and carrier concentration of ITO, AZO and i-ZnO films were measured by Vander Pauw method. Optical transmittance of ITO, AZO and i-ZnO was measured using UV-2401PC spectrophotometer from Shimadzu over a wavelength range of 300-1100nm. In order to make fundamental characterizations a 700 nm-thick graded CIGS film was deposited onto the glass substrate, using the pneumatic spray pyrolysis at typically 350^0C starting from metal (Cu, In, Ga) chlorides and n, n di-methyl selenourea as precursors. Cu:(Ga+In):Se atomic ratio in the solution was maintained as 1:1:3.5. An excess of dimethyl selenourea was taken in the starting solution in order to compensate the loss of selenium during the deposition due to its high vapour pressure. Finally graded CIGS layer was deposited over glass/(ITO or AZO)/ZnO after slight etching using buffered oxide etch (BOE) (NH_4F:HF) solution. X-ray diffraction (XRD) measurements have been performed on a PANalytical X-ray diffractometer with CuK_α (λ=1.5406Å) radiation.

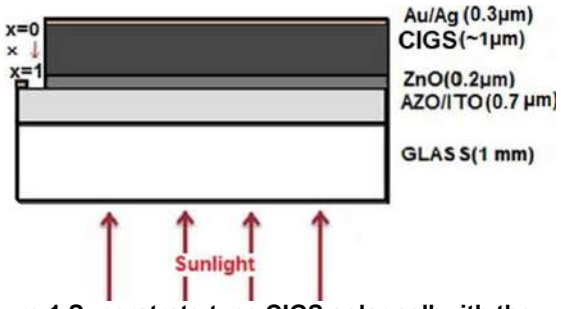

Figure 1 Superstrate-type CIGS solar cell with the glass/ITO (or) ZnO:Al/ZnO/CIGS/Au structure.

Thickness and surface morphology of the samples has been studied by using a Carl Zeiss Auriga 39-16 Field Emission Scanning Electron Microscope (FE-SEM) with a resolution of 1 nm at 15kV attached with Bruker AXS EDAX detector. Raman analysis has been performed using Horiba Jobin Yvan with He-Ne Laser at a wavelength of 632nm. UV-VIS-NIR spectra for CIGS films have been taken with a Varian cary UV-VIS-NIR spectrophotometer (300 - 3000nm). I-V measurements were performed using Keithley 6487 picoammeter/voltage source and Lakeshore 330 auto tuning temperature controller.

RESULTS AND DISCUSSION

XRD pattern of ITO (see Fig. 2 (a)) and ITO/ZnO (see Fig. 2 (b)) exhibits polycrystalline nature with a cubic phase of In_2O_3 [11] and hexagonal wurtizite phase of ZnO [5]. Characteristic 2θ lines at 21.4, 30.5, 35.3, 50.9, and 60.5° appeared as reflections from (2 1 1), (2 2 2), (4 0 0), (4 4 0), and (6 2 2) planes, respectively, which matched well with the card PDF #74-1990. No phases corresponding to tin oxide or to other tin compounds were detected in the XRD patterns. This can be attributed to the incorporation of Sn into the In_2O_3 lattice, consequently single-phase ITO films is formed. Upon i-ZnO deposition reflections at 34.3, 47.4, 62.7° appeared from (002), (102) and (103) planes respectively, matching with the card PDF #36-1451. XRD spectra of AZO (see Fig. 3(a)) and AZO/ZnO (see Fig. 3 (b)) shows polycrystalline hexagonal wurtizite structure with reflections at 34.3, 36.19, 47.4 and 62.7° appeared from (002), (101), (102) and (103) planes respectively, matching with the card PDF #35-1451. A peak corresponding to (101) plane is prominent in AZO compared to i-ZnO. No phases corresponding to aluminum oxide or to other aluminum compounds were detected in the XRD patterns, which can be attributed to the incorporation of Al into the ZnO lattice. FE-SEM images (see Fig. 4) of ITO(a), AZO(b), ITO/ZnO(c) and AZO/ZnO(d) clearly indicate that the films were dense and uniform without any pin hole or defects. Thicknesses of the layers were measured using cross-sectional images (see Fig. 4(c) and 4(d)). Line scan data for ITO/ZnO interface (see Fig. 5) revealed little or no interdiffusion, allowing the use of high temperatures for further deposition of CIGS. Composition values obtained from EDAX is given in table 1.

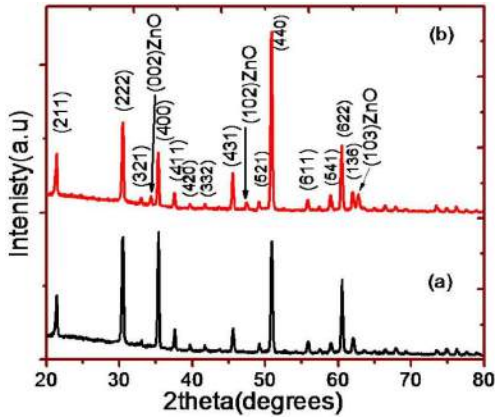

Figure 2 XRD spectra of ITO (a) and ITO/ZnO (b).

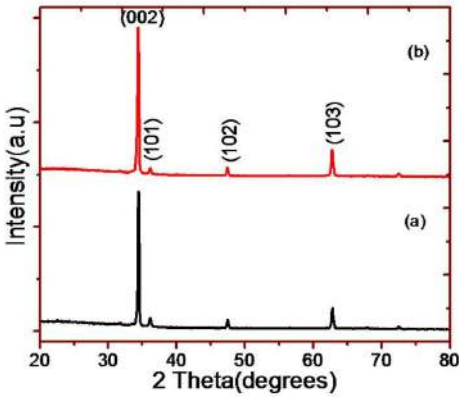

Figure 3 XRD spectra of AZO (a) and AZO/ZnO (b).

Resistivity, mobility, and carrier concentration of ITO, AZO and i-ZnO films were measured by Vander Pauw method and given in table 2. When Sn^{4+} replaced In^{3+} ions, Sn atoms entered substitutionally in the sublattice and acted as n-type donors [13]. Similarly Al^{3+} replaces Zn^{2+} ions [6], since the electron donors is more in ITO compared to that of AZO as given in table 2.

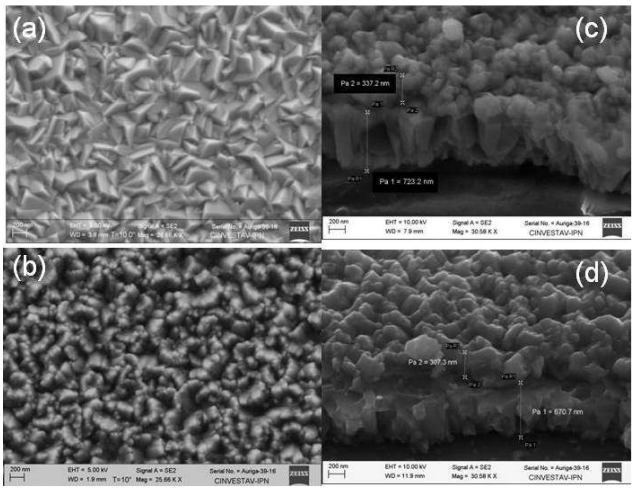

Figure 4 FE-SEM images of ITO(a), AZO(b), ITO/ZnO(c) and AZO/ZnO(d).

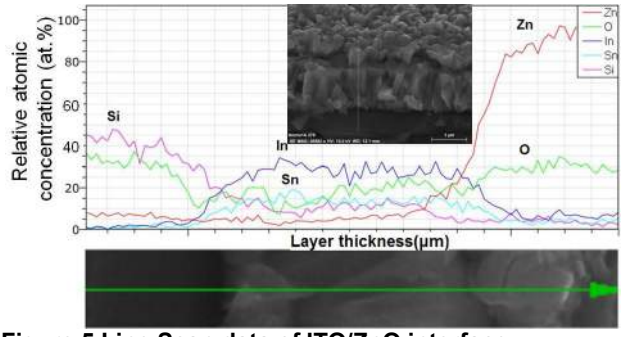

Figure 5 Line Scan data of ITO/ZnO interface.

Material	In/Zn(at%)	O(at%)	Sn/Al(at%)
ITO	33.45	64.77	1.77
AZO	49.38	50.12	0.50

Table 1 Composition of ITO and AZO layers.

Transmittance data for ITO(see Fig. 6 (a)), ITO/ZnO(see Fig. 6 (b)), AZO(see Fig. 7 (a)) and AZO/ZnO(see Fig. 7 (b)) showed >80%T, >55%T, >75%T and >65%T transmittance respectively in the visible region at 600nm. ITO on glass shows an absorption edge at 300 nm, however, the ZnO/ITO on glass presents a red-shift towards longer wavelength and shows an absorption band near 360 nm [11]. Similarly AZO and AZO/ZnO showed absorption edge at 368 nm. Inset figures (see Fig. 6 and 7) show their respective optical band gap values. Optical transmission decreases as ZnO is deposited over ITO and AZO, which is attributed to the optical scattering arising from longer optical paths and also to the increased carrier concentration in the films [12]. For ITO crystalline material with carrier concentration in the order $n \approx 10^{20}–10^{21}$ cm^{-3}, ionized impurity scattering can become more important than grain boundary scattering to limit the carrier mobility. Thus, the increased resistivity observed for the thicker layers is probably due to the increase in the scattering effect on free carriers from ionized impurities that are released due to the diminution of the grain boundary concentration [12].

Preliminary deposition of $Cu(In_{1-x}Ga_x)Se_2$ (x=1 to 0) on glass substrate yielded chalcopyrite phase (see Fig. 8) with a preferred (112) orientation. Other strong peaks observed from the XRD spectra correspond to the (220)/(204), (116)/(312) and (316)/(332) orientations. In addition to these lattice planes, one more peak corresponding to (103) plane was also seen in the films which exhibit the presence of chalcopyrite structure.

Material	Resistivity, ρ (Ohm-cm)	Mobility, μ (cm^2/V.s)	Concentration, n (cm^{-3})
ITO (723nm)	2e-4	28.61	1.08e+21
ITO/ZnO(1μm)	2.2e-4	33.42	8.30e+20
AZO (726nm)	5.7e-3	3.9	2.81e+20
AZO/ZnO(1μm)	3.4e-3	6.0	2.97e+20
i-ZnO (307nm)	43.69	3.4	4.81e+16

Table 2 Electrical parameters of ITO, AZO and i-ZnO layers.

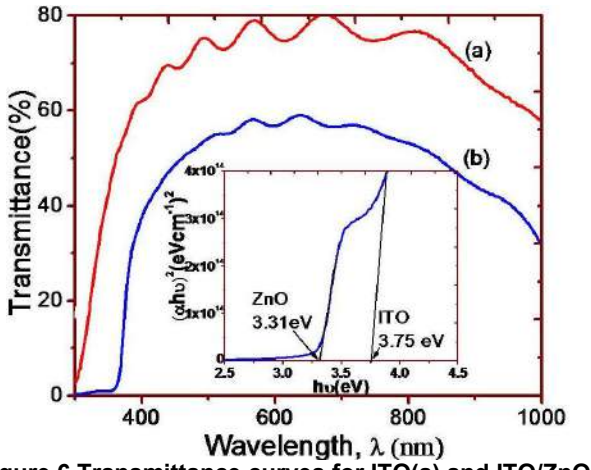

Figure 6 Transmittance curves for ITO(a) and ITO/ZnO (b).

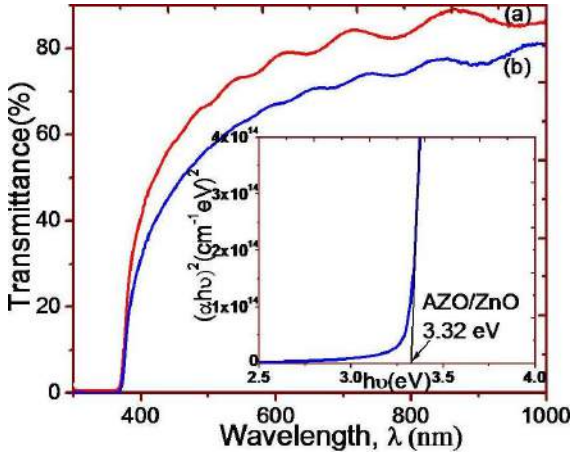

Figure 7 Transmittance curves for AZO (a) and AZO/ZnO (b).

An inset figure (see Fig. 8) indicates a clear tetragonal splitting of the (316)/(332) peaks which is a characteristic of the chalcopyrite structure. Lattice parameters a=5.77Å and c=11.84Å showed that the film is tetragonal nature. The splitting of doublet peak indicates the deviation of tetragonality, c/a= 2.05, induced by Ga substitution [8, 10]. Raman studies (see Fig. 9) showed a peak corresponding to A1 mode CIGS phase at 170 cm^{-1} with an asymmetric shape, and there seems to be a tail at higher frequency side.It is known that CIGS usually grown with mixed phase of chalcopyrite (CH) ordering and CuAu (CA) ordering, where A1 peak of CH and CA ordering is located at ~170 cm^{-1} and at ~178 cm^{-1} respectively. No other peaks corresponding to CuSe phase or any secondary phase were present. CIGS films grown using spray pyrolysis usually grow with mixed phase of chalcopyrite (CH) ordering and CuAu (CA) ordering [10]. For improvement of film quality of spray deposited CIGS films, higher substrate temperature may be desirable as it is reported for the growth of $Cu(InGa)Se_2$ [14]. However, we had some difficulties related with growth rate in growing spray pyrolysis CIGS films at higher temperatures.

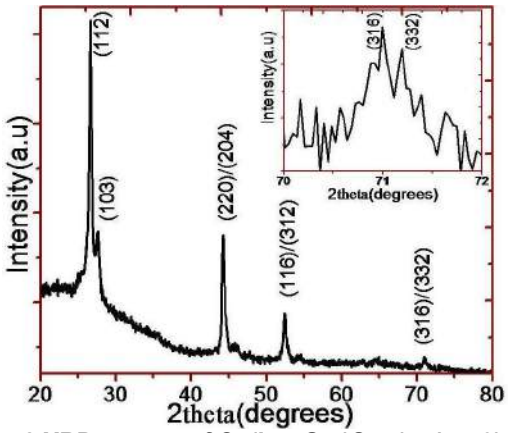

Figure 8 XRD pattern of $Cu(In_{1-x}Ga_x)Se_2$ (x=1 to 0) thin film.

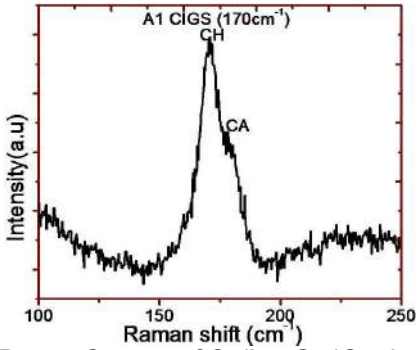

Figure 9 Raman Spectra of $Cu(In_{1-x}Ga_x)Se_2$ (x=1 to 0) thin film.

A 700 nm graded CIGS layer showed high optical absorption coefficient value of 6×10^6 cm^{-1} at a wavelength of 750nm with a band gap of 1.25 eV (see Fig. 10). FESEM image of graded CIGS layer (see Fig.11 (a)) and it's cross sectional image (see Fig.11 (b)) shows a dense and thick (700nm) layer. Line scan (see Fig. 11(c)) shows a decrease in Ga/(Ga+In) ratio from bottom layer to top layer, revealing graded nature of the film. Cu/(In+Ga) ratio varies from 0.77 to 1.06 from bottom to top. This layer shows an electrical resistivity of 0.49 Ω-cm, mobility of 4.20 cm^2/V.s and carrier concentration of 3×10^{18} cm^{-3}. In order to determine the activation energy for the saturation current, log (I) is plotted versus the inverse thermal voltage, 1/kT (see fig. 12)(a modified Arrhenius plot). In the case of CIGS film on glass, Arrhenius plot of the saturation current I_0 shows a linear dependence with activation energy E_A. Activation energy of the CIGS to glass is 0.49 eV(see Fig. 12), while it is 0.5 eV on CIGS/ZnO as reported by F.J. Haug [15] et. al. This graded CIGS layer is grown on ITO/ZnO and AZO/ZnO after slight etching of ZnO layer using BOE solution at room temperature, subsequently followed by cleaning with methanol and drying using nitrogen gas. After depositing CIGS, a 300 nm gold contact is deposited using thermal evaporation. XRD pattern of ITO/ZnO/CIGS (see Fig. 13(a)) and AZO/ZnO/CIGS (see Fig. 13 (b)) exhibits polycrystalline nature of the films.

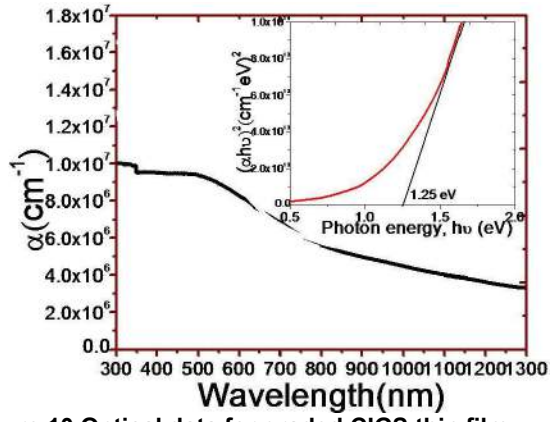

Figure 10 Optical data for graded CIGS thin film.

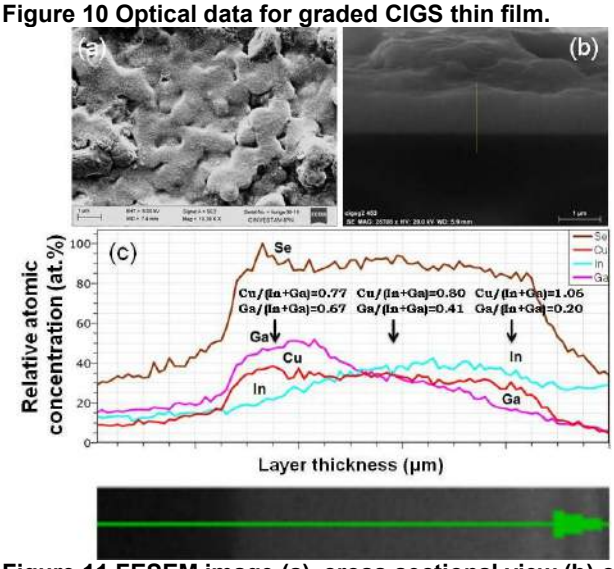

Figure 11 FESEM image (a), cross sectional view (b) of CIGS layer and its line scan (c).

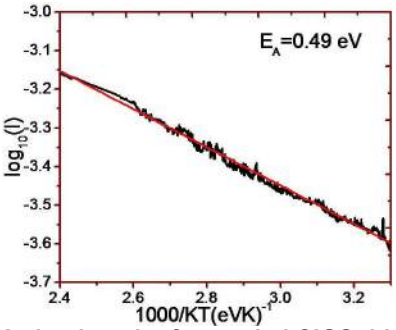

Figure 12 Arrhenius plot for graded CIGS thin film.

All the reflections found for the films were identified as planes corresponding to In_2O_3, ZnO and CIGS. But two reflections at 25.46 and 37.45° related to planes (101) and (211) respectively of Cu_3Se_2 phase. Chemical composition obtained for top layer i.e., CIGS film from EDAX on both devices is shown in table. 3. CIGS film on ITO/ZnO and AZO/ZnO showed Ga/(Ga+In) as 0.21 and 0.29 respectively. However CIGS film on AZO/ZnO has slightly Cu-rich and Se-deficient.

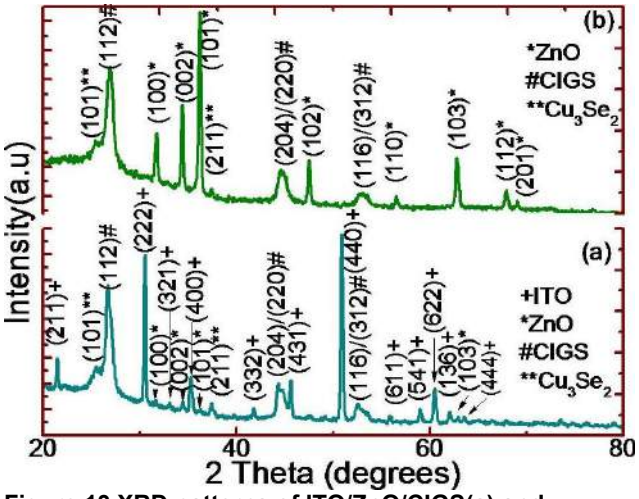

Figure 13 XRD patterns of ITO/ZnO/CIGS(a) and AZO/ZnO/CIGS(b).

Device	Cu at%	In at%	Ga at%	Se at%	Molecular Formula
ITO/ZnO /CIGS	24.79	18.49	5.07	51.65	$Cu_{0.96}(In_{0.79}Ga_{0.21})_{0.91}(se_{2.00})_{2.08}$
AZO/ZnO /CIGS	26.12	17.45	7.03	49.40	$Cu_{1.05}(In_{0.71}Ga_{0.29})_{0.99}(se_{2.00})_{1.89}$

Table 3 Chemical composition of CIGS layer on ITO/ZnO and AZO/ZnO junctions.

Cross sectional images of ITO/ZnO/CIGS/Au (see Fig. 14(a)) and AZO/ZnO/CIGS (see Fig. 14 (b)) gives thickness of the devices. Approximately 800 nm thick CIGS film is grown on 1 μm ITO/ZnO and AZO/ZnO layers. Line mapping of these devices reveal the elements present in each layer and no or little inter-diffusion is noticed at the junctions. As layer thickness increases in CIGS region, gallium gradient can be noticed which confirms the graded CIGS structure.

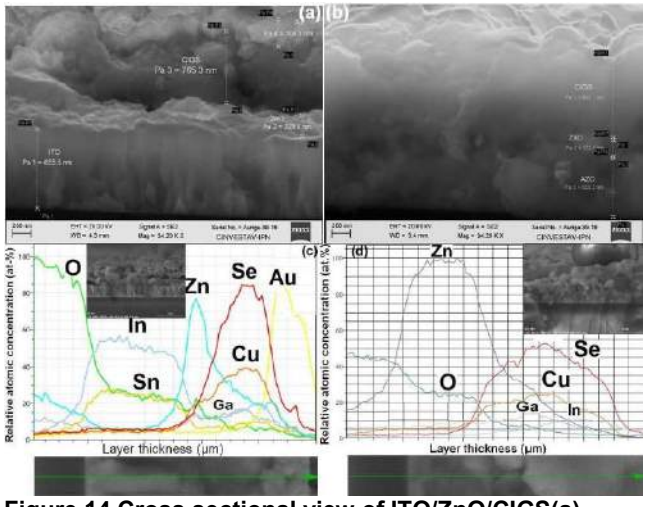

Figure 14 Cross sectional view of ITO/ZnO/CIGS(a) and AZO/ZnO/CIGS(b), its respective line scans (c) and (d).

More uniform layer was grown due to slower spray rates (6.5 ml/min) and surface topography of the films was found to be uniform with densely packed crystallites. Selenium content in the $Cu(In_{1-x}Ga_x)Se_2$ films was nearly equal to its stoichiometric value in the compound as mentioned in table.3, although an excess of selenium was taken in the starting solution. This may be because of the re-evaporation of selenium from the film surface during the deposition due to its high vapour pressure as the layers were formed at a temperature of 350°C [8]. All the CIGS films grown have shown an intersection of relative atomic concentration of gallium and indium taken by EDAX (see Fig. 11 and Fig. 14). As can be seen line profiles from this figures, the Ga/(In + Ga) decreased rapidly from 0.67 to 0.20, suggesting the formation of a graded band gap CIGS absorber layer. Grading of the Ga/(In + Ga) atomic ratio was intentionally formed by controlling Ga and In concentrations in the solutions during CIGS deposition. The beneficial effect of such grading on conversion efficiency (19.2%) has been addressed by Ramanathan [16] et. al. A recent study by Lundberg [17] et al. shows that the bandgap grading can increase the Voc by 20–30mV. It should be noted that at higher temperatures (550°C) Ga segregates at the ZnO/CIGS interface, presumably resulting in the formation of a highly resistive n-type Ga_2O_3 thin layer [2, 3]. However, the Ga_2O_3 that formed between CIGS and i-ZnO layers did not lead to a deterioration of the cell performance in the case of devices prepared for co-evaporation by Nakada [2, 3] et. al., since the undoped ZnO in the glass/ZnO:Al/ZnO/CIGS/Au structure was highly resistive. In contrast, no Ga segregation was observed for the CIGS/ZnO/AZO or CIGS/ZnO/ITO sample deposited at a substrate temperature of 350°C in the present study. Average Ga/(In+Ga) ratio in the CIGS films grown on ITO/ZnO and AZO/ZnO is 0.21 and 0.29 respectively, and that of Cu/(In+Ga) is 1.05 and 1.06 respectively.

These results clearly demonstrate the feasibility of preparing the CIGS based superstrate solar cell structure entirely by spray technique without need for a high temperature process or high vacuum. Optical response of this films and the cut-offs of the curve show the approximate band gap of ITO, ZnO and CIGS films. Spray-deposited films have defects, and extensive research is required to optimize the experimental conditions to yield better device quality structure, taking into consideration that CIGS is a promising candidate for thin film large-area solar cells. Annealing and selenization to the mentioned devices are underway and efficiency calculations are expected at the earliest.

CONCULSIONS

A graded $Cu(In_{1-x}, Ga_x)Se_2$ thin films with chalcopyrite structure were successfully deposited over ITO/ZnO and AZO/ZnO bilayers using a low cost non vacuum chemical spray pyrolysis technique. Low resistive and high transmittance films of ITO and AZO films were grown using ultrasonic spray pyrolysis. FE-SEM analysis also

showed pyramidal and columnar structure for ITO and AZO, ZnO. From these results, we inferred that ITO and AZO thin films may have better light trapping and antireflection effect. Gallium grading in the CIGS layers deposited on glass and ZnO is confirmed by line profiles obtained from EDAX. Unwanted secondary phases such as Ga_2O_3 at the ZnO/CIGS junction were not formed. Average Ga/(In+Ga) ratio in the CIGS films grown on ITO/ZnO and AZO/ZnO is 0.21 and 0.29 respectively. The present study demonstrated that $Cu(In_{1-x}, Ga_x)Se_2$ layers with gallium grading can be grown by spray pyrolysis which may be useful for solar cell application due to the low cost and simplicity of the technique.

ACKNOWLEDGEMENT

The authors wish to thank for technical assistance of Dr. Jaime Vega Perez, Ing. Adolfo Tavirce Fuentes. And our special thanks to Dr. A. Maldonado for providing USP facility also to Dr. Miguel Garcia Sanchez of UAM-I for UV-Vis-NIR measurements. B. J. Babu is thankful to CONACYT for the scholarship provided to pursue Doctoral program.

REFERENCES

[1] ZSW press release 11/2010, New world record with efficient CIGS solar cell, Zentrum fur Sonnenenergie-und Wasserstoff-Forschung Baden-Württemberg (ZSW) Stuttgart, Germany, 23 August 2010.

[2] T. Nakada, Y.Hirabayashi, T. Tokado, D. Ohmori, and T. Mise, "Novel device structure for Cu(In, Ga)Se_2 thin film solar cells using transparent conducting oxide back and front contacts", Solar energy **77**, 2004, pp. 739-747.

[3] T. Nakada and T. Mise, "High-efficiency superstrate type CIGS thin film solar cells with graded bandgap absorber layers", 17th European Photovoltaic Solar Energy Conference, Munich, 2001.

[4] F. J. Haug, D. Rudmann, G. Bilger, H. Zogg, and A.N. Tiwari, "Comparision of structural and electrical properties of Cu(In, Ga)Se_2 for substrate and superstrate solar cells", Thin Solid Films **403-404,** 2002, pp. 293-296.

[5] M. S. Tomar and F. J. Garcia, "A ZnO/p-$CuInSe_2$ Thin film Solar Cell prepared entirely by Spray Pyrolysis", Thin Solid Films **90,** 1982, pp. 419-423.

[6] B. J. Babu, A. Maldonado, S. Velumani and R. Asomoza, "Electrical and Optical properties of Ultrasonically Sprayed Al doped Zinc oxide thin films", Materials Science and Engineering B **174,** 2010, pp. 31–37.

[7] Sho Shirakata, Yoshiaki Kannaka, Harufumi Hasegawa, Tetsuya Kariya, and Shigehiro Isomura, "Properties of Cu(In,Ga)Se_2 Thin Films Prepared by Chemical Spray Pyrolysis," Jpn. J. Appl. Phys. **38 (1) No. 9A**, 1999, pp. 4997–5002.

[8] K. T. Ramakrishna Reddy and R. B. V. Chalapathy, "Structural Properties of $CuGa_xIn_{1-x}Se_2$ Thin Films Deposited by Spray Pyrolysis," Cryst. Res. Technol. **34 (1)**, 1999, pp. 127-132.

[9] B.J. Babu, S. Velumani, Arturo Morales-Acevedo and R. Asomoza, "Properties of CuInGaSe Thin Films Prepared by Chemical Spray Pyrolysis", 7th International Conference on Electrical Engineering Science, Computing Science and Automatic control, Tuxtla Gutiérrez, Chiapas, México, 2010.

[10] Dong-Yeup Lee, SeJun Park and JunHo Kim, "Structural analysis of CIGS film prepared by chemical spray deposition", Current Applied Physics **11,** 2011, pp. S88-S92.

[11] Chueh-Jung Huang, Wen-Kai Chao and Fuh-Sheng Shieu, "Characteristics of Zinc Oxide Crystallites Deposited on ITO for Dye-sensitized Solar Cells", J. Chin. Chem. Soc. **57, No. 5A**, 2010, pp. 1.

[12] C. Guillén and J. Herrero, "Polycrystalline growth and recrystallization processes in sputtered ITO thin films", Thin Solid Films **510,** 2006, pp. 260–264.

[13] Jiaxiang Liu, Da Wu and Shengnan Zeng, "Influence of temperature and layers on the characterization of ITO films", Journal of materials processing technology, **209,** 2 009, pp. 3943-3948.

[14] Sho Shirakata, Yoshiaki Kannaka, Harufumi Hasegawa, Tetsuya Kariya and Shigehiro Isomura, "Properties of Cu(In,Ga)Se2 Thin Films Prepared by Chemical Spray Pyrolysis", Jpn. J. Appl. Phys. **38,** 1999, pp. 4997–5002.

[15] F.J. Haug, D. Rudmann, A. Romeo, H. Zogg, and A. N. Tiwari, "Electrical properties of the heterojunction in Cu(In,Ga)Se_2 superstrate solar cells", 3rd World Conference on Photovoltaic Solar Energy Conversion, Osaka, 2003.

[16] Kannan Ramanathan, Miguel A. Contreras, Craig L. Perkins, Sally Asher, Falah S. Hasoon, James Keane, David Young, Manuel Romero, Wyatt Metzger, Rommel Noufi, James Ward and Anna Duda, "Properties of 19.2% Efficiency ZnO/CdS/CuInGaSe2 Thin-film Solar Cells", Prog. Photovolt: Res. Appl. **11,** 2003, pp. 225–230.

[17] Lundberg O, Bodegard M, Malmstrom J and Stolt L, "Influence of the Cu(In,Ga)Se_2 thickness and Ga grading on solar cell performance" Progress in Photovoltaics: Research and Applications **11,** 2003, pp. 77–88.